

DETERMINATION OF CUTTING FORCES USING A FLEXURE-BASED DYNAMOMETER: DECONVOLUTION OF STRUCTURAL DYNAMICS USING THE FREQUENCY RESPONSE FUNCTION

Michael F. Gomez and Tony L. Schmitz
 Department of Mechanical Engineering and Engineering Science
 University of North Carolina at Charlotte
 Charlotte, NC

INTRODUCTION

Accurate measurement of cutting forces is fundamental to the understanding and modeling of machining processes. Traditionally, cutting force measurements are performed using a multi-axis piezoelectric-based cutting force dynamometer. A workpiece is mounted on the dynamometer, which is mounted to the machine table and aligned with the feed direction [1]. However, the dynamic properties of the dynamometer must be considered when operating at or near the dynamometer's natural frequencies. At the natural frequencies there is an artificial amplification of force signals which can lead to inaccurate force readings. The cutting force measurements can be corrected by filtering the measured forces using the dynamometer force-to-input force transmissibility [2-4]. In doing so, there is a structural deconvolution of the unwanted dynamometer dynamics from the measured force signals.

This paper presents a novel method for cutting force measurement using displacement of a flexure-based dynamometer. In this case, the structural deconvolution is carried out by applying a filter to measured vibration signals based on the flexure's inverted frequency response function (FRF).

STRUCTURAL DECONVOLUTION

A simulation was programmed in MATLAB® to demonstrate the deconvolution of the structural dynamics for a single degree of freedom (SDOF) system. The first step in performing the deconvolution is to measure the structure's FRF. This was completed by impact testing, where an instrumented hammer is used to excite the structure and a measurement transducer is used to record the resulting vibration [1]. Using the system's FRF (see Fig. 1) the differential equation of motion in response to a harmonic forcing function takes the form:

$$m\ddot{x} + c\dot{x} + kx = A \sin(\omega t) \quad (1)$$

where, m , c , and k are the modal mass, damping, and stiffness parameters obtained from the FRF, A

is force magnitude, and ω is the forcing frequency. The solution to the differential equation was obtained in this study by time-domain simulation; example results are displayed in Fig. 2.

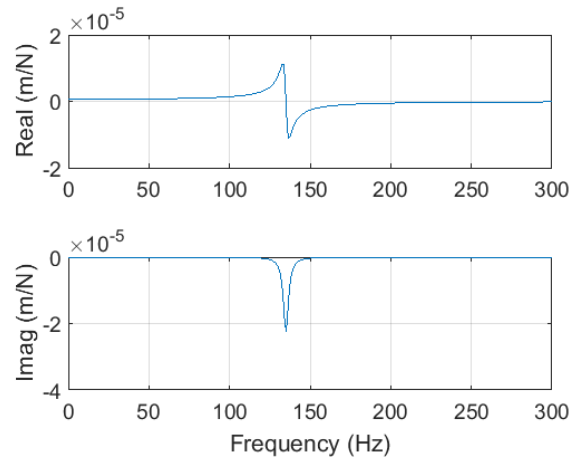


Figure 1: Real and imaginary parts of the FRF for the simulated SDOF system. The natural frequency, f_n , of the system is 135 Hz.

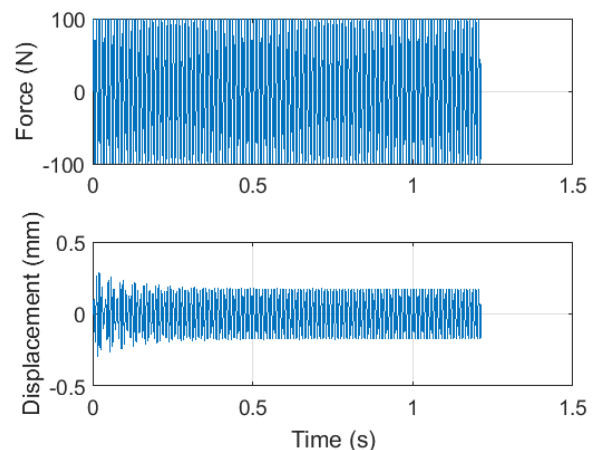


Figure 2: Time-domain response of a SDOF system (bottom) to the force profile (top). The displacement was calculated using Euler integration.

The inverted FRF is used to generate a filter which is applied to the frequency-domain displacement to

determine the frequency-domain force; see Fig. 3. The force is then transformed back into the time-domain. As a result, the force is based on displacement, rather than the traditional piezoelectric signal.

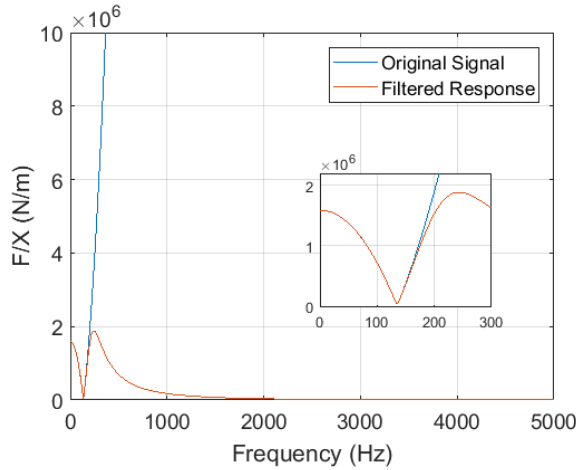


Figure 3: Frequency-domain response of the inverse filter used to remove the influence of the SDOF system dynamics. A low-pass 4th order Butterworth filter is applied to remove the effects of high-frequency content.

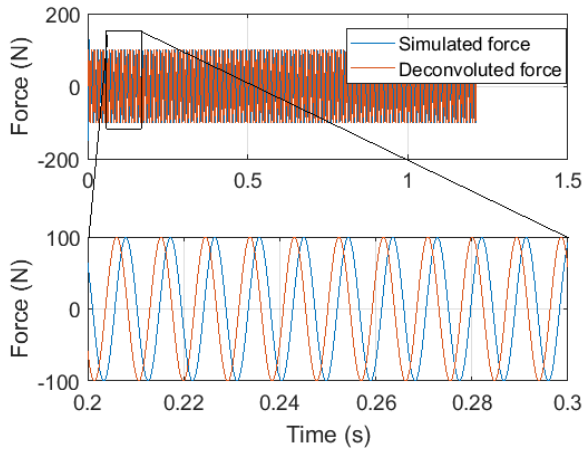


Figure 4: Time-domain comparison of simulated and calculated forces obtained by structural deconvolution.

Figure 4 demonstrates the technique for an ideal displacement signal. The results closely agree. To investigate the effects of noise, a 5% noise level was added to the force and displacement signals. The results are shown in Fig. 5. The structural deconvolution method is adversely affected by noise levels. Therefore, a high signal-to-noise ratio is necessary in order to obtain accurate results.

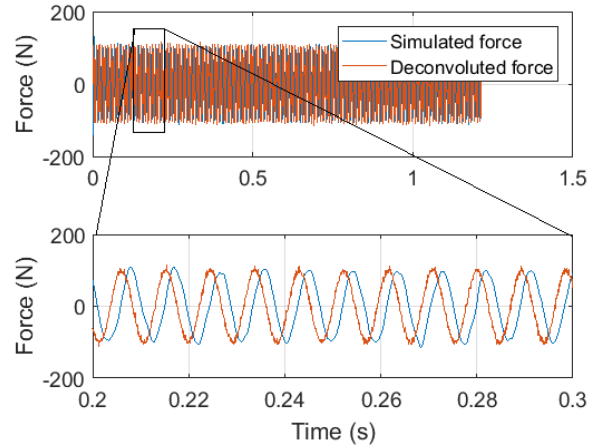


Figure 5 : Time-domain response of a SDOF system. A 5% noise level was added to the force and displacement signals.

EXCITATION FORCE MEASUREMENT

A series of tests were performed in order to compare measured and calculated forces. The SDOF flexure dynamics are provided in Table 1.

Table 1: SDOF Flexure dynamics.

f_n [Hz]	Damping ratio	k [N/m]
134.0	0.029	1.66×10^6

A function generator (Tektronix AFG 3022B) was used to command a waveform input for a modal shaker (TV 51075-M), which then excited the SDOF flexure system through a stinger (the stinger supports axial tension and compression, but not bending or shear [5]). A piezoelectric load cell (PCB 086C04) was affixed to the flexure end of the stinger to measure the excitation force applied to the system. The flexure vibrations were measured using a capacitance probe (LION Precision C-18-13-2.0). The experimental setup is illustrated in Fig. 6.

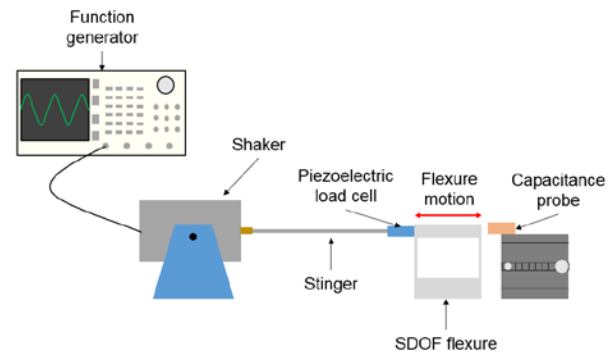


Figure 6: Flexure-based dynamometer experimental setup with a capacitance probe and modal shaker. Note that the excitation direction is in-line with the flexible direction of the flexure.

A series of waveforms were used to illustrate the ability to reproduce excitation forces via structural deconvolution. The commanded waveforms are described in Table 2.

Table 2: Commanded waveforms produced by the function generator and shaker.

Waveform	Forcing frequency [Hz]
Sine	5
Ramp	5
Square	20
Gaussian	50

While the sine and ramp waves contain only the fundamental forcing frequency, the square and Gaussian waves contain additional frequency content at integer multiples of the forcing frequency. The results of this experiment are shown in Figs. 7-10.

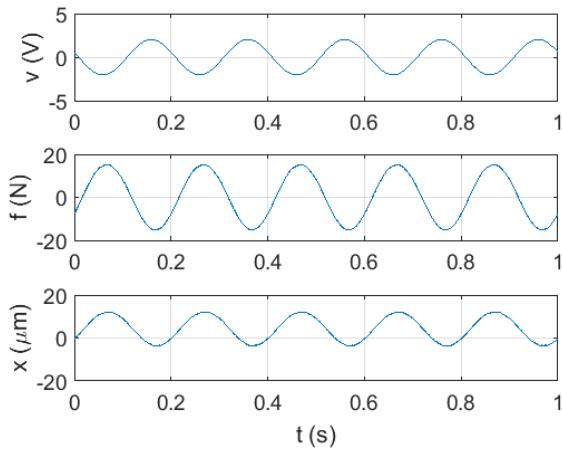


Figure 7: Time domain signals for a commanded sine wave at 5 Hz. The commanded sine wave (top), the measured force by the piezoelectric load cell (middle), and the measured displacement by the capacitance probe (bottom).

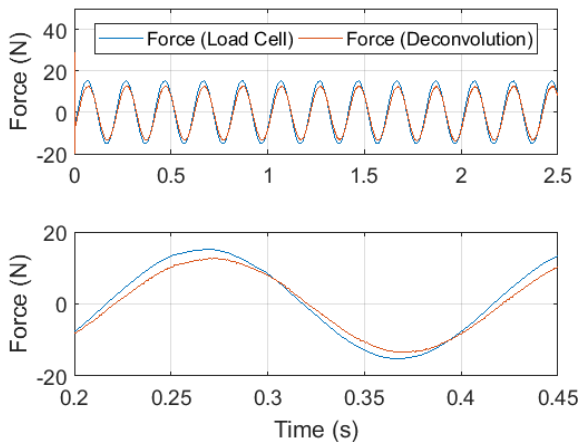


Figure 8: Time-domain comparison of measured and calculated forces for a sine wave with a forcing frequency of 5 Hz.

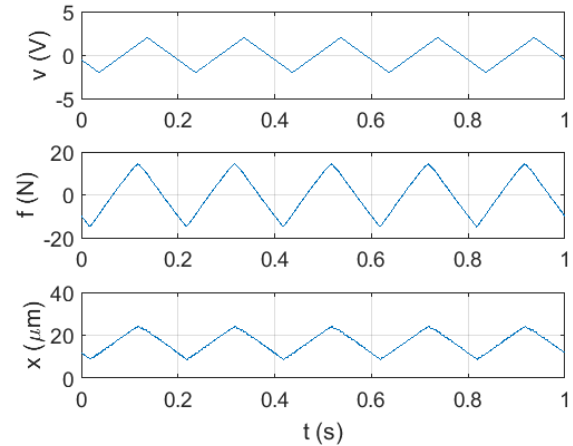


Figure 9: Time-domain signals for a commanded ramp wave at 5 Hz.

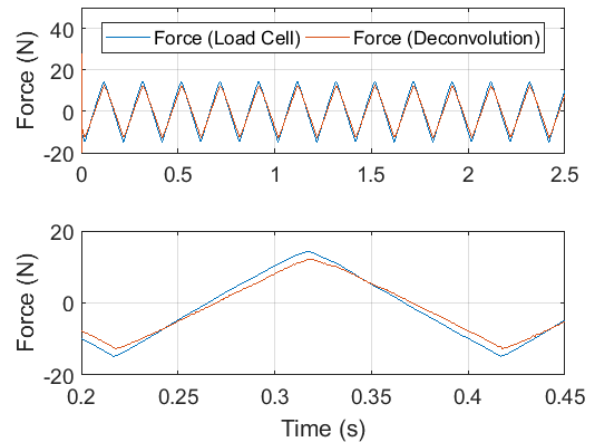


Figure 10: Time-domain comparison of measured and calculated forces for a ramp wave with a forcing frequency of 5 Hz

Frequently, partial radial immersion cutting forces resemble trains of periodic impulses [5]. Therefore, square and Gaussian waves were used to simulate the forces that may be encountered during milling experiments; see Figs. 11 and 13. A 4th order low-pass Butterworth filter was applied to the inverse flexure FRF with a cut-off frequency equal to the 10th harmonic (multiple) of the forcing frequency.

The forces were successfully reconstructed with minor discrepancies in the amplitude, as shown by Figs. 12 and 14. The differences in amplitude can be attributed to the low-pass filter which attenuates higher-order frequencies which may be present in the forcing function.

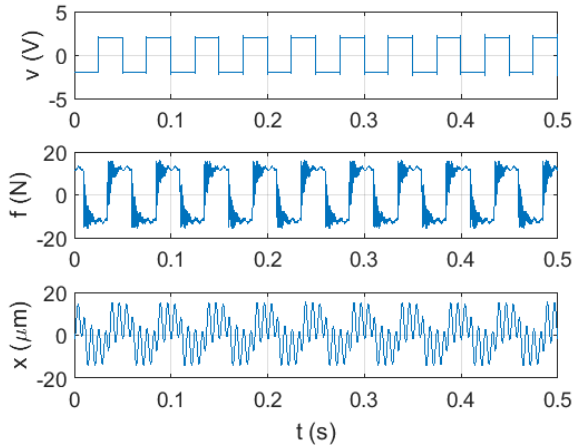


Figure 11: Time-domain signals for a commanded square wave at 20 Hz and a 50% duty cycle.

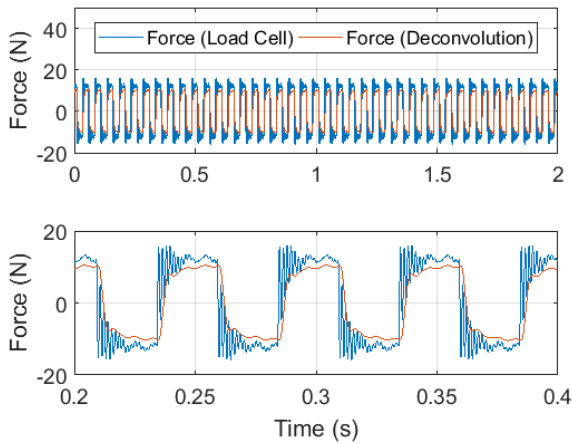


Figure 12: Time-domain comparison of measured and calculated forces for a square wave with a forcing frequency of 20 Hz.

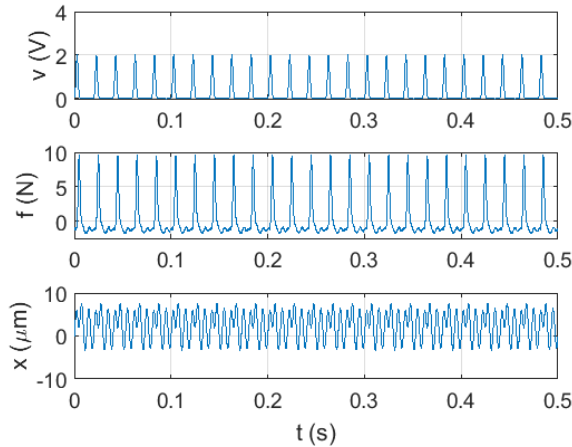


Figure 13: Time-domain signals for a commanded Gaussian wave at 50 Hz.

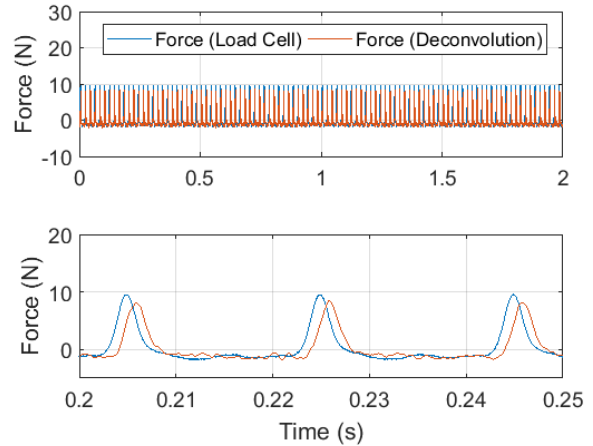


Figure 14: Time-domain comparison of measured and calculated forces through structural deconvolution. There is good agreement between the measured and calculated forces.

The measured and calculated force frequency content for the Gaussian waveform is shown in Fig. 15. It can be observed that the structural deconvolution replicates the fundamental frequency and its harmonics until the relative amplitudes are substantially dissipated. Further, the frequency-domain is useful in observing any added effects from the piezoelectric load cell.

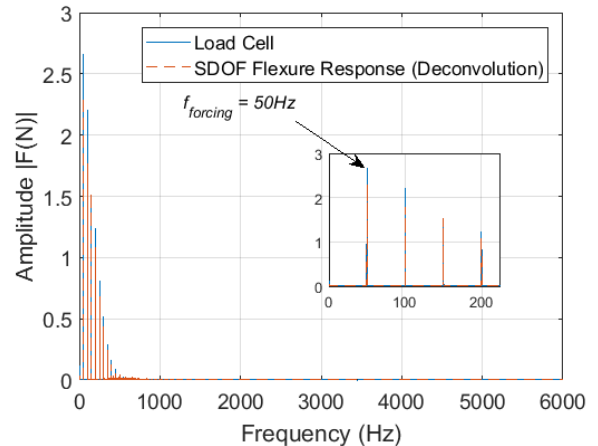


Figure 15: Comparison of the frequency content for the measured and calculated forces.

CUTTING FORCE MEASUREMENT

The first set of cutting tests were carried out by mounting an aluminum workpiece on a multi-axis dynamometer (Kistler Type 9257B). The second set of cutting tests were performed by mounting the workpiece on the SDOF flexure, where the flexure displacement was measured using a capacitance probe (LION Precision C-18-13-2.0); see Fig. 16. It is important to note that the measurement transducer

was aligned with the flexible direction of the SDOF flexure.

Stable down-milling machining conditions were selected for all trials at a spindle speed of 2550 rpm. The radial and axial depths of cut were both 2 mm. A set of three feed rates were chosen for this study: {25, 75, and 125} $\mu\text{m}/\text{tooth}$.

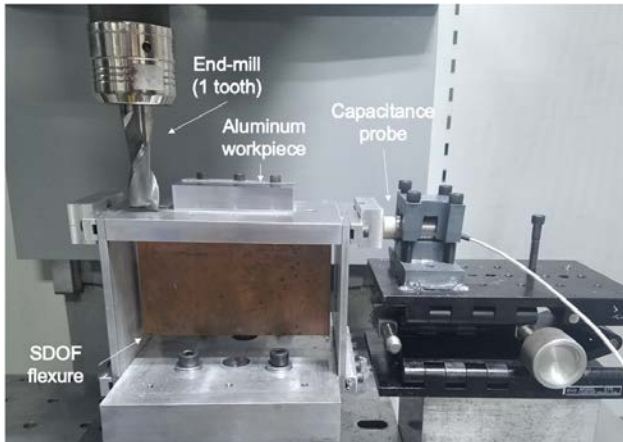


Figure 16: Flexure-based dynamometer experimental setup with a capacitance probe. Note that the feed direction is in-line with the flexible direction of the flexure.

RESULTS

The magnitude and coherence of the FRF for the SDOF flexure-dynamometer is shown by Fig. 17. The FRF was generated by an impact test using a modally tuned hammer (PCB 086C04 SN29958) and its displacement response was measured using the capacitance probe.

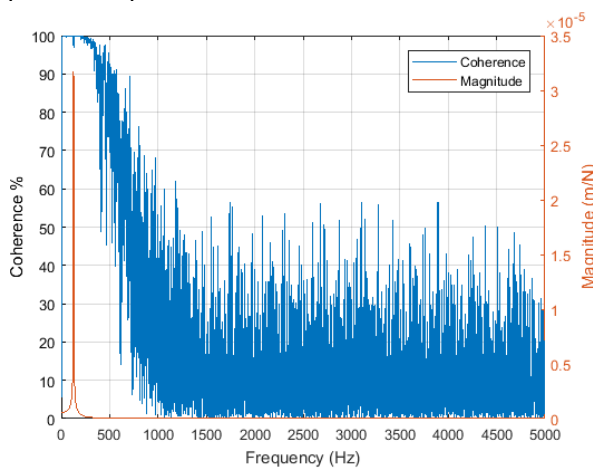


Figure 17: Magnitude and coherence measurements for the single degree of freedom flexure system used for the generation of cutting forces.

A comparison of the force signals is shown in Figs. 18-20. The displacement signal of the SDOF flexure was used to calculate cutting forces. Further, a low-pass filter was applied to the measured cutting forces

to attenuate the high frequency content introduced by the dynamometer. These initial results show good agreement between the flexure-based dynamometer and the piezoelectric-based dynamometer.

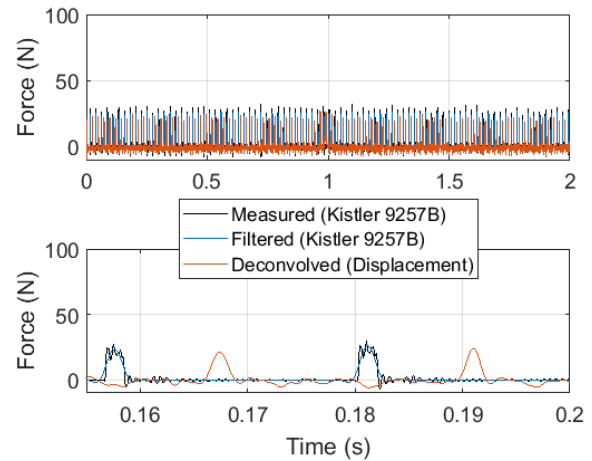


Figure 18: Measured, filtered, and calculated cutting forces for the 25 $\mu\text{m}/\text{tooth}$ test.

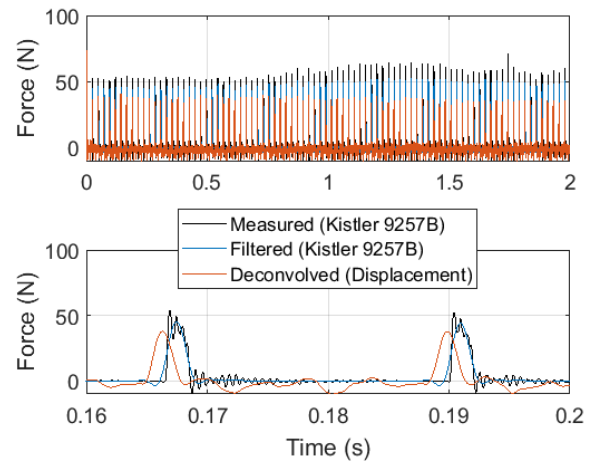


Figure 19: Measured, filtered, and calculated cutting forces for the 75 $\mu\text{m}/\text{tooth}$ test.

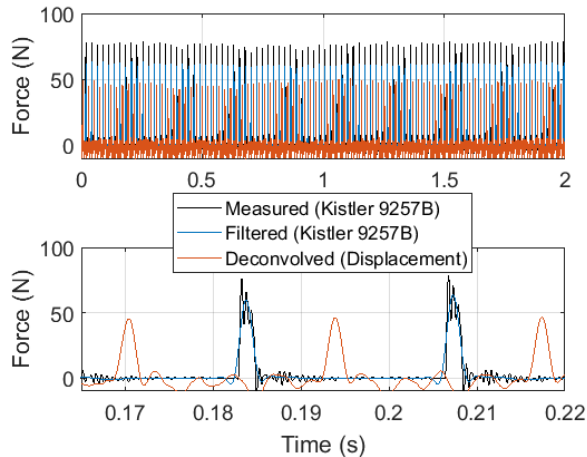


Figure 20: Measured, filtered, and calculated cutting forces for the 125 $\mu\text{m}/\text{tooth}$ test.

The frequency content for the measured and calculated cutting forces is shown in Fig. 21. The additional frequency content introduced by the dynamometer structural response serves to artificially amplify the measured cutting forces at higher frequencies.

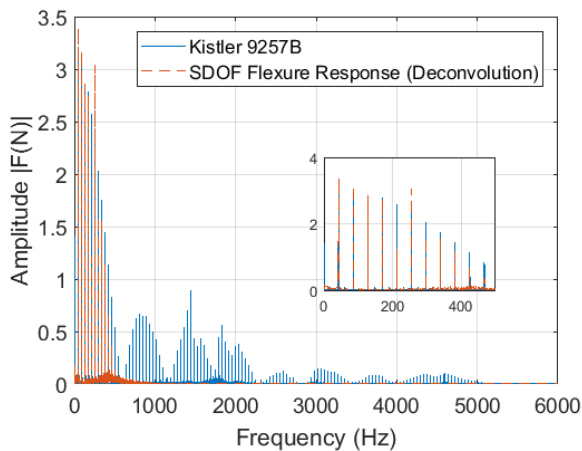


Figure 21: Cutting force frequency content for the Kistler 9257B dynamometer and the SDOF flexure-based dynamometer.

CONCLUSIONS

The purpose of this paper was to demonstrate the ability to measure cutting forces using the displacement of a flexure-based dynamometer. In this case, the structural deconvolution was carried out by applying a filter to a measured displacement signal based on the flexure's inverted frequency response function. It was shown that, for a variety of excitation forces, the measured displacement can be used to reconstruct the force profile.

It was found that it is important to consider the signal-to-noise ratio for the displacement transducer because the displacement-to-force frequency domain analysis is sensitive to noise. A low-noise displacement sensor is therefore necessary to accurately reconstruct the excitation force.

REFERENCES

- [1] Schmitz T. L. and Smith K. S. (2009). *Machining Dynamics: Frequency Response to Improved Productivity*. Springer, New York, NY
- [2] Korkmaz E., Gozen B. A., Bediz B., Ozdoganlar O. B. (2015). High-Frequency Compensation of Dynamic Distortions in Micromachining Force Measurements. *Procedia Manufacturing* 127: 673-678.
- [3] Castro L. R., Vieville P., Lipinski P. (2006). Correction of dynamic effects on force measurements made with piezoelectric dynamometers. *International Journal of Machine Tools and Manufacture* 46: 1707-1715.
- [4] Rubeo, M. A. and Schmitz T. L. (2016). Mechanistic force model coefficients: A comparison of linear regression and nonlinear optimization. *Precision Engineering* 45: 311-321.
- [5] Schmitz T. L. and Smith K. S. (2012). *Mechanical Vibrations: Modeling and Measurement*. Springer, New York, NY